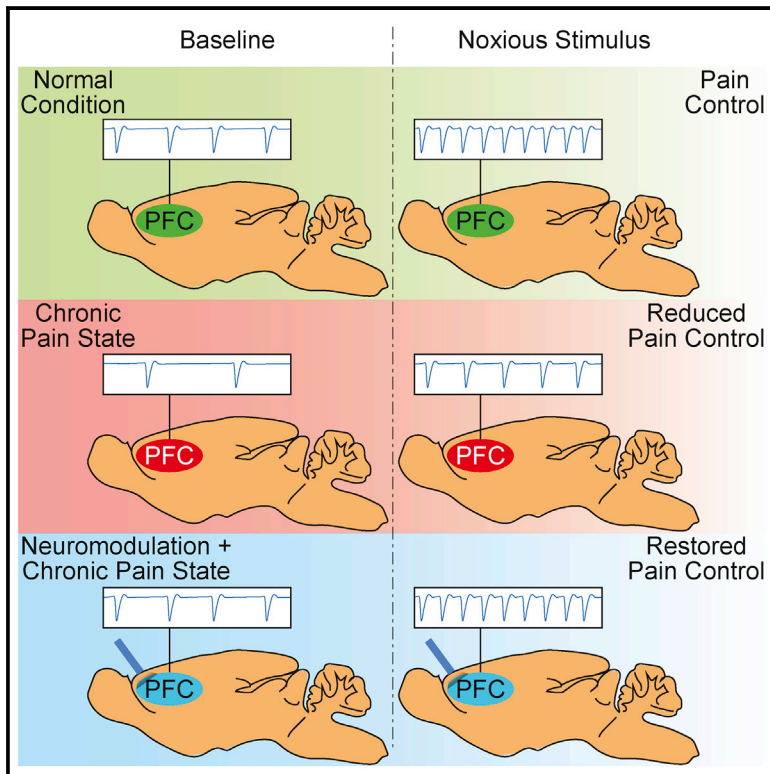


Scaling Up Cortical Control Inhibits Pain

Graphical Abstract



Authors

Jahrane Dale, Haocheng Zhou, Qiaosheng Zhang, ..., Louise Urien, Zhe Chen, Jing Wang

Correspondence

jing.wang2@nyumc.org

In Brief

Dale et al. find that acute pain increases activity levels in the prefrontal cortex. Chronic pain reduces both basal spontaneous and pain-evoked activity in this region, whereas neurostimulation to restore basal activities can in turn enhance nociception-evoked prefrontal activities to inhibit pain.

Highlights

- Acute pain increases the firing rates of neurons in the prefrontal cortex (PFC)
- There is a correlation between basal and pain-evoked firing rates in the PFC
- Chronic pain decreases both basal spontaneous and pain-evoked firing rates in the PFC
- Increasing basal prefrontal firing rates can enhance the gain of cortical pain control



Scaling Up Cortical Control Inhibits Pain

Jahrane Dale,^{1,5} Haocheng Zhou,^{1,2,5} Qiaosheng Zhang,¹ Erik Martinez,¹ Sile Hu,³ Kevin Liu,¹ Louise Urien,¹ Zhe Chen,^{3,4} and Jing Wang^{1,4,6,*}

¹Department of Anesthesiology, Perioperative Care and Pain Medicine, New York University School of Medicine, New York, NY, USA

²Department of Pain, The Third Xiangya Hospital and Institute of Pain Medicine, Central South University, Changsha, Hunan Province, China

³Department of Psychiatry, New York University School of Medicine, New York, NY, USA

⁴Department of Neuroscience and Physiology, New York University School of Medicine, New York, NY, USA

⁵These authors contributed equally

⁶Lead Contact

*Correspondence: jing.wang2@nyumc.org

<https://doi.org/10.1016/j.celrep.2018.03.139>

SUMMARY

Acute pain evokes protective neural and behavioral responses. Chronic pain, however, disrupts normal nociceptive processing. The prefrontal cortex (PFC) is known to exert top-down regulation of sensory inputs; unfortunately, how individual PFC neurons respond to an acute pain signal is not well characterized. We found that neurons in the prelimbic region of the PFC increased firing rates of the neurons after noxious stimulations in free-moving rats. Chronic pain, however, suppressed both basal spontaneous and pain-evoked firing rates. Furthermore, we identified a linear correlation between basal and evoked firing rates of PFC neurons, whereby a decrease in basal firing leads to a nearly 2-fold reduction in pain-evoked response in chronic pain states. In contrast, enhancing basal PFC activity with low-frequency optogenetic stimulation scaled up prefrontal outputs to inhibit pain. These results demonstrate a cortical gain control system for nociceptive regulation and establish scaling up prefrontal outputs as an effective neuromodulation strategy to inhibit pain.

INTRODUCTION

Pain is a salient sensory stimulus that elicits neural responses to protect us from injury (Basbaum et al., 2009). Chronic pain, however, disrupts normal nociceptive processing in peripheral and central neurons, giving rise to sensory hypersensitivity and enhanced aversion (Basbaum et al., 2009; Li et al., 2010; Navratilova et al., 2012). Restoring or improving endogenous regulation of acute pain may be an effective way to relieve chronic pain.

The prefrontal cortex (PFC) is an important center for top-down regulation of sensory inputs (Salzman and Fusi, 2010). Stimulation of the PFC can inhibit withdrawal reflexes and aversive responses to pain (Hardy, 1985; Kiritoshi et al., 2016; Lee et al., 2015; Martinez et al., 2017; Zhang et al., 2015). Imaging studies in patients with chronic pain have shown, however, that the PFC undergoes structural alterations (Apkarian et al., 2004; Geha et al., 2008; Moayedi et al., 2011). *In vitro* studies in animal models have further demonstrated decreased excit-

ability of prefrontal neurons under chronic pain conditions, as the result of impaired glutamate, endocannabinoid, and cholinergic signaling (Ji and Neugebauer, 2011; Kelly et al., 2016; Radzicki et al., 2017; Zhang et al., 2015). These studies raise the possibility that chronic pain causes neurons in the PFC to become deficient in their ability to regulate nociceptive inputs. The understanding of nociceptive processing in the PFC, however, has been limited by a lack of knowledge about how individual neurons respond to a noxious stimulus *in vivo*. Furthermore, it is not known how this response to noxious stimulation is impaired by chronic pain. Finally, our understanding of cortical pain processing is hindered by the lack of a mechanism that can link changes at the cellular level to disrupted nociceptive regulation at the network level.

In the present study, we provide for the first time a detailed characterization for how neurons in the PFC respond to acute pain signals in awake, free-moving rats. We found that a significant number of neurons in the prelimbic region of the PFC (PL-PFC) increased their firing rates (FRs) in response to acute pain. Chronic pain, however, lowered both basal spontaneous firing and pain-evoked FRs in the PL-PFC. Furthermore, we found that basal firing and pain-evoked FRs are positively correlated on a linear scale; hence, a small change in basal firing leads to a much larger alteration in the neural response to pain. Enhancing basal firing of PFC neurons with low-frequency optogenetic stimulation, meanwhile, scaled up prefrontal outputs and inhibited pain. Therefore, we propose a cortical gain control mechanism. PFC neurons can function as gain controllers for pain, and scaling down the gain of nociceptive regulation by suppressing the basal excitability of PFC neurons represents a key pathologic feature in chronic pain. Conversely, scaling up prefrontal control with low-frequency stimulation may be a novel neuromodulation strategy to treat pain and related neuropsychiatric diseases.

RESULTS

Neurons in the PFC Increase Their FRs in Response to Peripheral Noxious Stimulations

To understand how the PFC responds to a painful stimulus, we used tetrodes to measure the FRs of neurons in the PL-PFC before and after noxious stimulations (with pinpricks [PPs]) of the contralateral hind paws of awake, free-moving rats (Figures 1A and 1B). PPs produced reliable nociceptive withdrawal



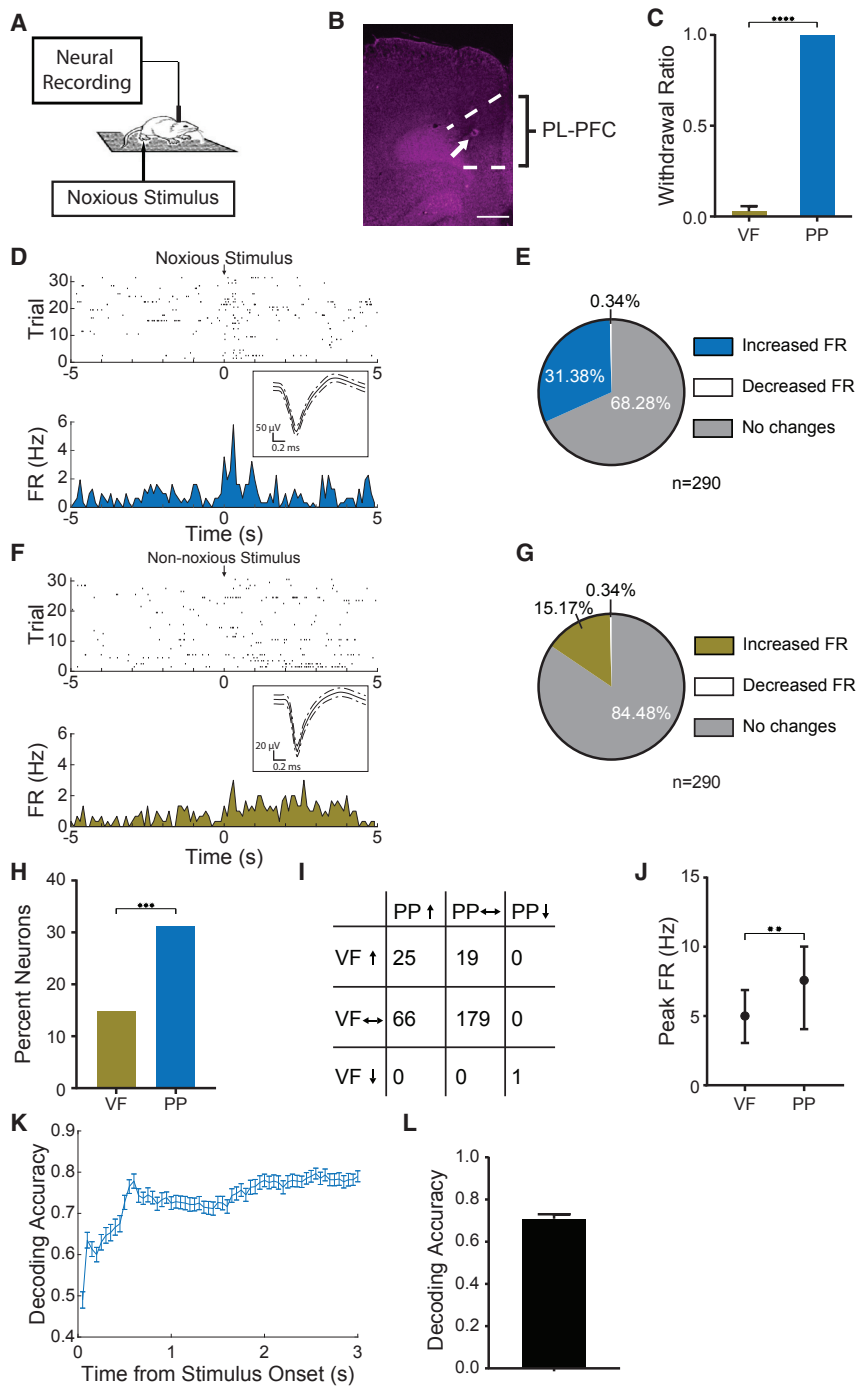


Figure 1. Neurons in the PFC Increase Firing Rates in Response to an Acute Pain Stimulus

(A) Experimental paradigm for electrophysiological recordings in free-moving rats. Neural activities in the PFC were recorded before and after peripheral noxious stimulation (with PP using a 28G needle) to the hind paw through a mesh table. Each trial lasted until paw withdrawal.

(B) Histology showing the location of recording tetrodes in the prelimbic PFC contralateral to peripheral stimulations. Scale bar, 1,000 μ m.

(C) PP caused nocifensive paw withdrawals, in contrast to stimulation with a non-noxious stimulus using 2-g VF filament. $n = 7$, $p < 0.0001$, paired Student's t test.

(D) Raster plots and PSTHs of a representative prefrontal neuron. Time 0 indicates the onset of noxious (PP) stimulation. Inset shows representative single-cell recordings. FRs, firing rates.

(E) A total of 31.38% of recorded neurons in the PFC ($n = 290$ from three rats) demonstrated increased FRs in response to acute pain (pain-responsive neurons). See [Experimental Procedures](#).

(F) Raster plots and PSTHs before and after non-noxious (VF filament) stimulation.

(G) A total of 15.17% of recorded neurons ($n = 290$) demonstrated increased FRs in response to VF filaments. See [Experimental Procedures](#).

(H) The difference in the proportion of neurons that increased their FRs in response to VF filaments and PP is statistically significant. $p = 0.0002$, Fisher's exact test. See [Experimental Procedures](#).

(I) Most of the neurons that respond to the mechanical pain stimulus (PP) did not respond to non-painful (VF filament) stimulation. \uparrow : neurons that increase their FRs; \downarrow : neurons that decrease their FRs; \leftrightarrow : neurons that did not alter their FRs in response to a peripheral stimulus. $p < 0.0001$, Fisher's exact test.

(J) In neurons that responded to both stimuli, PP induced higher FRs than VF filaments. $n = 25$, $p = 0.0011$, Wilcoxon paired signed-rank test. See [Experimental Procedures](#) for calculations of stimulus-evoked FRs.

(K) A representative session of unbiased SVM-based population-decoding analysis to distinguish between painful and non-painful stimulations. Time 0 denotes the stimulus (PP or VF filaments) onset. The blue curve denotes the decoding accuracy ($n_1 = 28$ trials for PP, $n_2 = 27$ trials for VF filaments; $C = 7$ PFC neurons) derived from the data with true labels; the error bar denotes the SEMs from 50 Monte Carlo simulations based on 5-fold cross-validation; the maximum decoding accuracy was 0.79. See [Experimental Procedures](#) for details.

(L) SVM-based population-decoding analysis demonstrated the ability to distinguish between painful and non-painful stimulation. $n = 20$ sessions from three rats. Data in (C), (K), and (L) are represented as mean \pm SEM. Insets in (D) and (F) are represented as mean \pm SD. Data in (J) are represented as medians with interquartile ranges. See also [Figure S1](#).

responses with short and well-defined latency (Figures 1C and S1A). We found that >30% of the neurons increased their FRs in response to this noxious stimulus (Figures 1D and 1E; see [Experimental Procedures](#) for the definition of pain-responsive neurons). Prefrontal neurons are multifunctional and can

respond to a variety of sensory and affective signals (Rigotti et al., 2013; Salzman and Fusi, 2010). Thus, to define the relative specificity of this pain-triggered response, we recorded these neurons in the context of non-noxious stimulations (with a von Frey [VF] filament) of the hind paws (Figures 1A–1C and 1F).

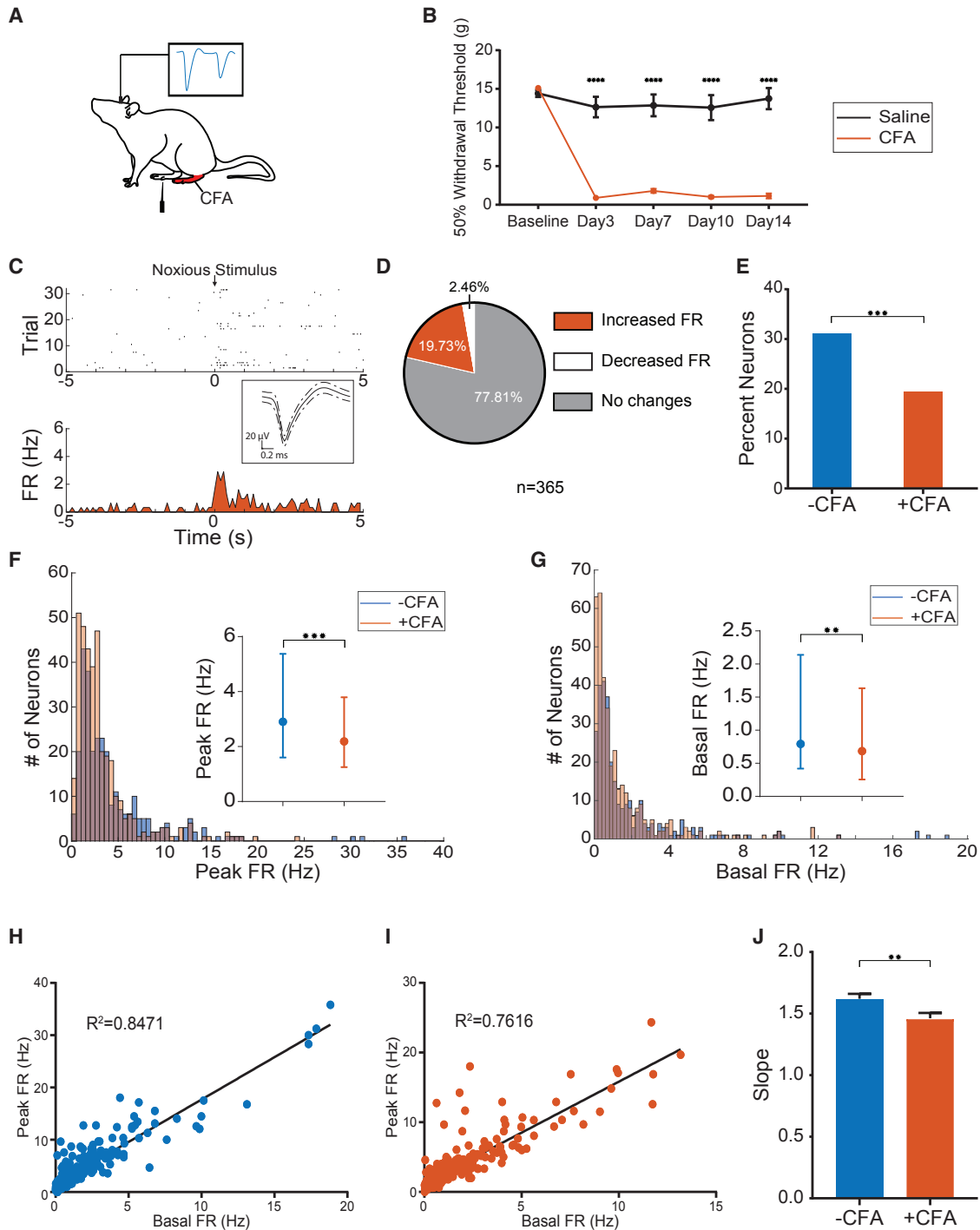


Figure 2. Chronic Pain Suppresses the Prefrontal Response to Acute Pain

(A) Schematic for recording nociceptive responses in the PFC in the chronic pain state. CFA was injected into the hind paw of a rat to induce persistent pain, and recordings were performed before and after peripheral stimulation of the contralateral, uninjected paw. Thus, CFA injection was ipsilateral to implanted recording electrodes.

(B) CFA induced chronic inflammatory pain, as indicated by mechanical allodynia in the affected limb. $n = 6$, $p < 0.0001$, two-way ANOVA with repeated measures and Bonferroni post-tests.

(C) Raster plot and PSTH of a representative prefrontal neuron in the chronic pain state.

(D) A total of 19.73% of recorded prefrontal neurons ($n = 365$ from three rats) responded to acute pain in the chronic pain state.

(E) Chronic pain reduced the number of pain-responsive neurons in the PFC. $p = 0.0007$, Fisher's exact test.

(legend continued on next page)

The number of neurons that responded to this non-painful stimulus was substantially smaller compared to the painful stimulus (Figures 1G and 1H). In addition, only 27% of the neurons (25 of 91) that responded to acute pain increased their FRs in the presence of the non-painful stimulus (Figure 1I). Furthermore, in neurons that responded to both painful and non-painful stimuli, pain elicited significantly higher FRs (Figure 1J). We then analyzed the duration and latency of neural responses in the PFC after PP and VF filament stimulations. We found that PPs on average elicited increased firing for a longer duration than VF filaments and that there also was a greater variation in the duration of the neural changes in the PFC after noxious stimulations than non-noxious stimulations (Figure S1B). In addition, the latency to neural response after PPs was significantly shorter than it was after VF filaments (Figure S1C). These results support the specificity of the response of individual neurons in the PFC to noxious stimulations. Finally, to examine whether population responses can differentiate between painful and non-painful stimuli, we applied an unbiased decoding analysis based on the support vector machine (SVM), using FRs of individual prefrontal neurons as features (Figures 1K and 1L). Our analysis yielded a peak decoding accuracy of 79%, further supporting the specificity of pain responsiveness of PFC neurons (see [Experimental Procedures](#) for details).

Chronic Pain Suppresses Basal Activities of Prefrontal Neurons as well as Their Responses to Acute Noxious Stimulations

Next, we examined whether the presence of chronic pain impairs the prefrontal response to acute pain. Previous studies have shown that chronic pain can enhance the FRs or synaptic function of neurons in the anterior cingulate cortex (ACC) in response to noxious stimulations, even if the stimulus is at a different location from the site of chronic pain (Li et al., 2010; Zhang et al., 2017). Thus, to generalize the relevance of our study to better understand prefrontal nociceptive regulation, we induced chronic pain at a site that was distinct from acute pain stimulations. We injected complete Freund's adjuvant (CFA) into the rats' hind paws ipsilateral to implanted tetrodes to induce chronic inflammatory pain (Figures 2A and 2B) and then measured prefrontal responses to acute mechanical pain in the uninjured hind paws contralateral to tetrode implants. In rats with chronic inflammatory pain, we continued to identify pain-responsive neurons in the PL-PFC (Figure 2C). However, the percentage of pain-responsive neurons in CFA-treated rats was reduced considerably, suggesting a deficit in the nociceptive response at the population level (Figures 2D and 2E). Furthermore, there was a significant reduction in pain-evoked FRs among all of the recorded neurons (Figure 2F), including acute

pain-responsive neurons in the PFC (Figure S2A). This decrease in the median FRs, along with the distinct distribution of the overall lower FRs of neurons in rats with chronic pain compared with naive rats, indicates a deficit in the nociceptive response at the level of individual prefrontal neurons.

Previous *in vitro* findings suggest the decreased excitability of neurons in the PFC in chronic pain models (Ji and Neugebauer, 2011; Kelly et al., 2016; Radzicki et al., 2017; Zhang et al., 2015). This hypoexcitability, however, has not been observed in free-moving animals. This hypoexcitability should manifest as decreased basal spontaneous FRs in our study. As expected, we found that chronic pain indeed decreased the spontaneous FRs of all of the recorded neurons (Figure 2G), including neurons that specifically responded to acute pain (Figure S2B).

The PFC Can Function as a Cortical Gain Control Center for Pain

Next, we analyzed the relation between basal and pain-evoked FRs in these prefrontal neurons. It is interesting that the spontaneous basal FRs of recorded neurons in awake free-moving animals were positively correlated with pain-evoked FRs, both in the absence and presence of chronic pain (Figures 2H and 2I). Qualitatively, these results indicate that the responsiveness of an individual prefrontal cell to pain correlates strongly with its basal activity level. Quantitatively, the slope of each linear correlation provides a ratio (>1.6 in naive rats) for the strength of the prefrontal output as a function of the basal activity level of individual neurons. Thus, any decline in basal FRs caused by decreased cellular excitability (Ji and Neugebauer, 2011; Kelly et al., 2016; Radzicki et al., 2017; Zhang et al., 2015) can result in an almost 2-fold decrease in sensory-evoked FRs. Because the output from the PFC can modulate acute pain (Hardy, 1985; Kiritoshi et al., 2016; Lee et al., 2015; Martinez et al., 2017; Zhang et al., 2015), our results indicate a prefrontal mechanism of gain control for pain regulation. The gain of the prefrontal modulatory output is determined by the basal FRs and the ratio between pain-evoked and basal FRs. We found that this ratio declined by 10% in the chronic pain state (Figure 2J). Therefore, chronic pain impairs prefrontal nociceptive control in two ways: through a decrease in basal excitability and through a decrease in the ratio between evoked and basal responses.

Enhancing Basal Activities Can Scale Up Prefrontal Responses to Acute Pain

Our results suggest a causal role for basal cellular activity to drive pain-evoked responses in the PFC. To test this causal relation, we used low-frequency (2 Hz) optogenetic stimulation to increase the basal firing of pyramidal neurons in the PL-PFC. We then used

(F) Chronic pain reduced pain-evoked FRs of prefrontal neurons. Left: histogram showing the distribution of neurons. Right: median \pm interquartile range for evoked FRs in rats with (red) or without (blue) chronic pain. $p = 0.0002$, Mann-Whitney U test.

(G) Chronic pain decreased the basal FRs of PFC neurons. Left: histogram showing the distribution of neurons. Right: median \pm interquartile range for basal FRs of PFC neurons. $p = 0.0071$, Mann-Whitney U test. See [Experimental Procedures](#) for calculations of basal FRs.

(H) Linear regression analysis shows a strong positive correlation between basal firing and acute pain-evoked FRs. See [Experimental Procedures](#). Slope = 1.621, $R^2 = 0.8471$.

(I) CFA-treated rats maintained a strong positive correlation between basal firing and pain-evoked FRs in PFC neurons. Slope = 1.463, $R^2 = 0.7616$.

(J) The difference in the slopes of the two linear regressions suggests a further decline in the ability to respond to acute pain signals in the chronic pain state. $p = 0.0077$, analysis of covariance (ANCOVA).

Data in (B) and (J) are represented as mean \pm SEM. Data in (C) are represented as mean \pm SD. See also [Figure S2](#).

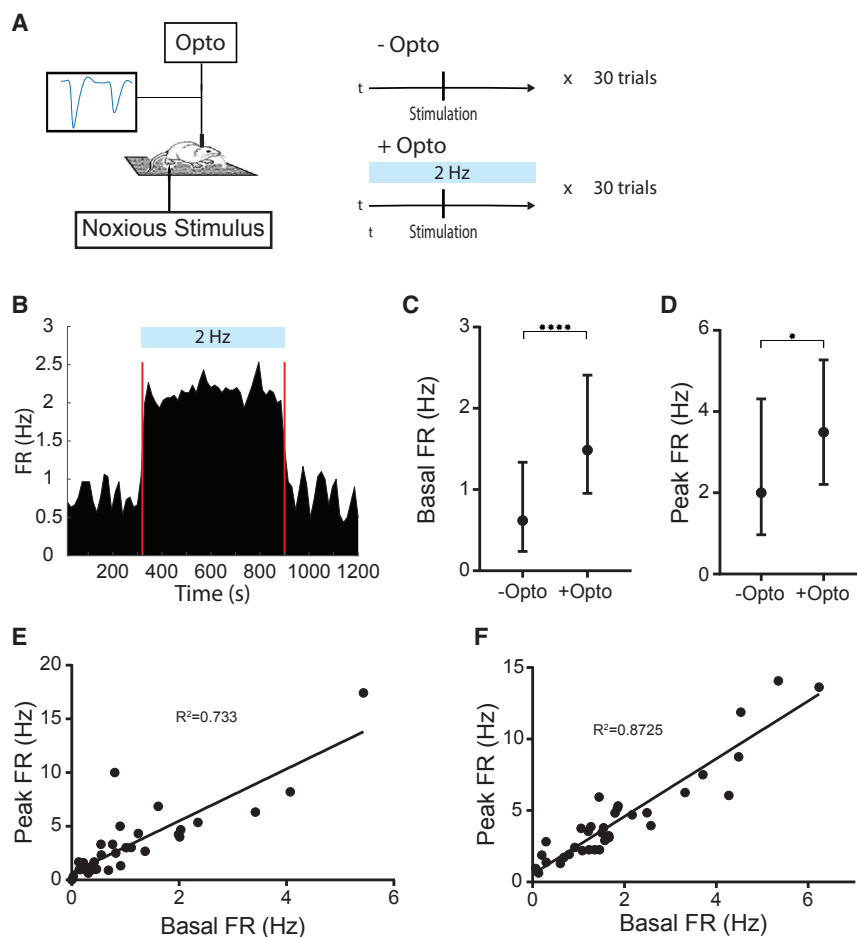


Figure 3. Increasing Basal Activities Can Scale Up the Prefrontal Response to Acute Pain

(A) Schematic for *in vivo* optrode recordings. (B) Representative recording trace shows that 2-Hz optogenetic stimulation increased the basal FRs of a pyramidal neuron in the PFC. (C) Low-frequency (2 Hz) optogenetic stimulation increased the basal FRs of a number of prefrontal neurons. $n = 36$ (out of a total of 69 from two rats), $p \leq 0.0001$, Wilcoxon paired signed-rank test. (D) Low-frequency (2 Hz) activation increased the FRs of prefrontal neurons in response to acute pain. $n = 36$, $p = 0.0421$, Wilcoxon paired signed-rank test. (E and F) The strong correlation between basal and pain-evoked FRs was preserved without (E) and with (F) optogenetic stimulation. Slope = 2.42, $R^2 = 0.733$ (E) and slope = 2.02, $R^2 = 0.8725$ (F). Data are represented as medians with interquartile ranges. See also Figure S3.

implanted optrodes to record the FRs of these neurons in response to acute pain (Figure 3A). Our optrode recordings demonstrated that low-frequency stimulation increased spontaneous basal FRs in approximately half of the neurons (Figures 3B and 3C). We then carefully examined the FRs of the select neurons that were activated by the low-frequency stimulation. These neurons with increased basal firing in turn demonstrated increased acute pain-evoked FRs (Figure 3D). These data showed that increasing basal firing can indeed scale up pain-evoked FRs. As expected, the significant positive correlation between basal FRs and evoked FRs was preserved among these neurons with increased basal FRs during optogenetic stimulation (Figures 3E and 3F). These results provide additional support for the role of PFC as a gain controller for pain. They also confirm that the ability of cortical neurons to respond to pain is causally dependent on their basal FRs in the awake state. Finally, these results raise the possibility that we can scale up, or amplify, endogenous cortical responses to pain by increasing basal excitability.

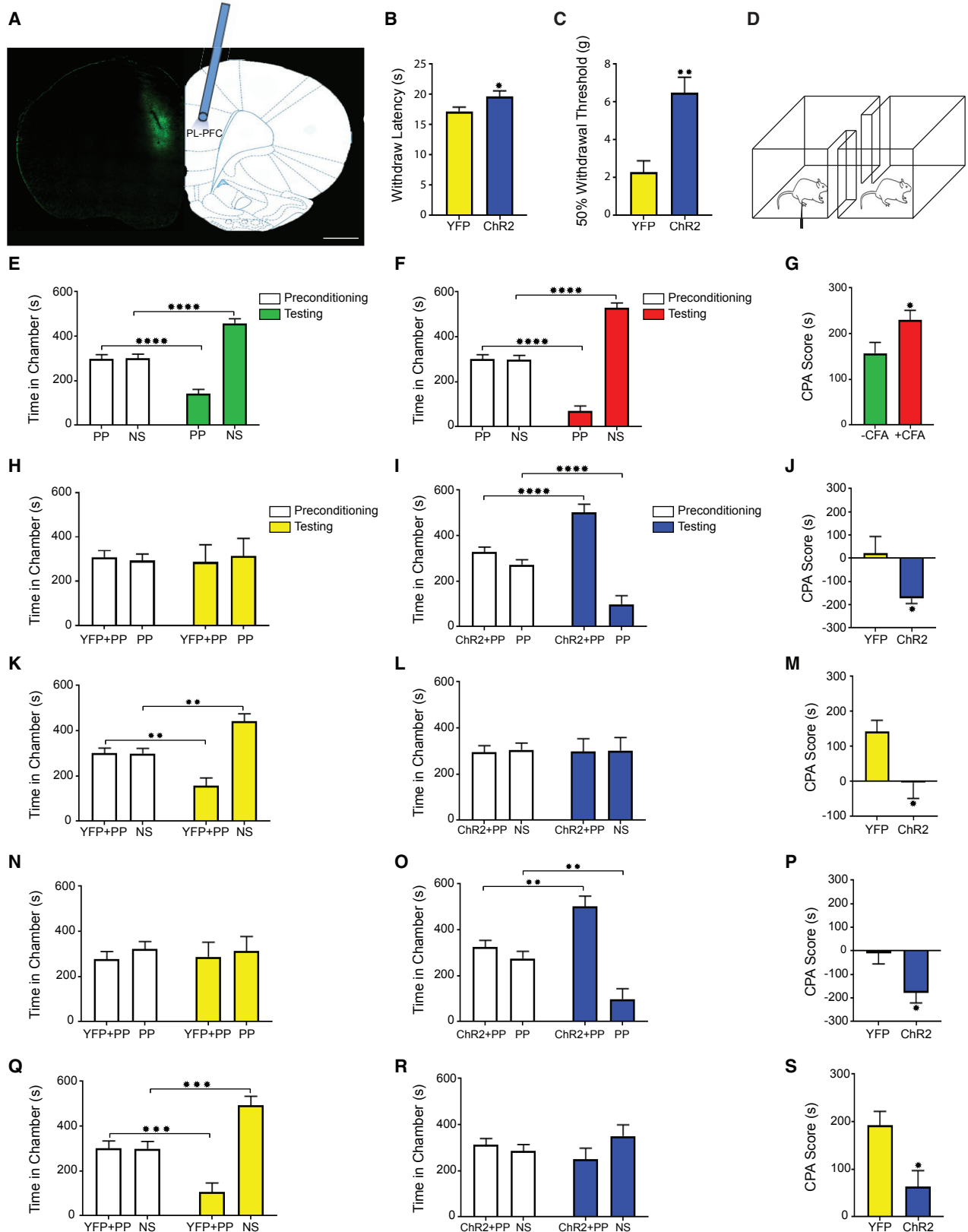
Scaling Up Prefrontal Outputs Can Inhibit Pain

Recent studies have demonstrated that supraphysiological activation of pyramidal neurons in the PFC can relieve pain (Kiritoshi et al., 2016; Lee et al., 2015; Martinez et al., 2017; Zhang et al., 2015). In contrast, our results suggest that a novel strategy is

to enhance basal activities in these neurons within the physiological range to increase the gain for endogenous regulatory outputs. To test this strategy, we used 2-Hz optogenetic stimulation to increase the basal FRs of pyramidal cells in the PL-PFC and measured the impact of this neurostimulation approach on pain-related behaviors (Figures 3, 4A, and S3). First, we examined sensory responses. We found that scaling up prefrontal outputs by increasing basal firing

provided effective inhibition of acute nociceptive withdrawals based on results from the Hargreaves test (Lee et al., 2015; Martinez et al., 2017) (Figure 4B). We then tested the effect of low-frequency prefrontal stimulation on a chronic pain (CFA) model. We found that augmenting basal activities in the PFC also provided relief of mechanical allodynia in CFA-treated rats (Figure 4C). These behavioral results suggest that scaling up prefrontal outputs by enhancing the basal activity level has antinociceptive effects in naive rats and rats with chronic pain.

We then investigated the impact of this neuromodulatory strategy on the aversive component of pain, using a well-established conditioned place aversion (CPA) assay (Figure 4D) (Johansen et al., 2001; King et al., 2009; Zhang et al., 2017). When rats were conditioned in one chamber with a noxious stimulus and the other chamber without it, they displayed aversion to the chamber associated with noxious stimulation (Figure 4E). Chronic pain has been shown to induce a generalized anatomically nonspecific increase in this aversive response to acute pain (Zhang et al., 2017). We calculated a CPA score by subtracting the amount of time that rats spent in the chamber paired with a noxious stimulus during the test phase from the time that they spent in that chamber at baseline (Johansen et al., 2001). A higher CPA score indicates a stronger aversive response. As expected (Zhang et al., 2017), compared to control rats, rats with



(legend on next page)

chronic pain displayed an increased aversive response to acute pain stimulation in the uninjured paws (Figures 4F and 4G).

We tested whether scaling up prefrontal outputs can modify these aversive phenotypes of pain. We paired one chamber with a noxious stimulus and 2-Hz activation of the PFC and the other chamber with that noxious stimulus alone. Rats preferred the chamber associated with increased basal prefrontal activities (Figures 4H–4J). Next, we paired one chamber with the noxious stimulus and low-frequency stimulation and the other chamber without the noxious stimulus. We found that rats did not avoid the chamber associated with noxious stimulation; thus, enhancing basal activities in the PFC reduced pain aversion (Figures 4K–4M).

Next, we examined the impact of scaling up prefrontal activities in rats with chronic pain. CFA-treated rats preferred the chamber associated with low-frequency optogenetic treatment when both chambers were paired with noxious stimulation (Figures 4N–4P). Furthermore, CFA-treated rats did not avoid the chamber associated with a painful stimulus, if that stimulus was coupled with enhanced prefrontal outputs (Figures 4Q–4S). Taken together, these results suggest that low-frequency stimulation, by restoring basal activities, can scale up prefrontal control to relieve the aversive quality of chronic pain. We did not observe any rewarding effect of low-frequency stimulation in the absence of noxious stimulation, nor did prefrontal stimulation alter locomotion (Figure S4), suggesting that enhancing basal prefrontal activities did not significantly alter baseline sensory and motor behaviors.

To further verify the specificity of this gain control mechanism for pain in prefrontal neurons, we inactivated the outputs from PL-PFC in naive rats by expressing halorhodopsin in their pyramidal neurons (Figure 5A). We then performed Hargreaves and CPA tests in the presence of PFC inactivation. We found that inactivation of the PFC decreased the latency to withdrawal on the Hargreaves test, suggesting that PFC inhibition had pro-nociceptive effects (Figure 5B). We then tested, using the CPA assay, the impact of PFC inhibition on the affective component of pain. We paired PFC inactivation with PPs in one chamber and PPs without PFC inactivation in the opposite chamber during conditioning. During the test phase, rats demonstrated aversion to the chamber associated with PFC inactivation (Figures 5C and 5D), as demonstrated by an elevated CPA score compared with yellow fluorescent protein (YFP)-treated (control) rats (Figure 5E). These results are compatible with our recorded neural data, which showed that a significant number of PFC neurons responded to acute pain stimuli. Taken together, they strongly suggest that PFC neurons at baseline exert crucial endogenous regulatory functions for pain-related behaviors, and thus they provide additional support for the role of the PFC as a gain controller for pain.

The PFC has multiple projections to other cortical and subcortical areas. To further demonstrate the behavioral specificity of our proposed cortical gain control mechanism at the circuit level, we selectively targeted neurons from the PL-PFC that project to neurons in the core region of the nucleus accumbens (NAc)

Figure 4. Increasing Basal Activities in the PFC Relieves Pain

(A) Histologic expression of ChR2-eYFP in the prelimbic PFC. Scale bar, 1000 μ m.

(B) Low-frequency (2 Hz) optogenetic activation of the PFC increased the latency to paw withdrawal on the Hargreaves test. $n = 11$ – 12 , $p = 0.0427$, unpaired Student's *t* test.

(C) Low-frequency activation of the PFC relieved mechanical allodynia. $n = 8$ – 11 , $p = 0.0014$, unpaired Student's *t* test.

(D) Schematic for a two-chamber CPA test to assess the aversive response to acute pain.

(E) Rats displayed aversive responses to acute mechanical pain. One of the chambers was paired with PP stimulation; the other chamber was not paired with a painful stimulus (NS). $n = 17$, $p < 0.0001$, paired Student's *t* test.

(F) Rats were injected with CFA in one hind paw, and the CPA test was conducted by conditioning with noxious stimulus in the opposite uninjured paw. $n = 17$, $p < 0.0001$, paired Student's *t* test.

(G) Chronic pain induced enhanced aversive response to acute pain, demonstrated by an increase in the CPA score. $n = 17$, $p = 0.0377$, paired Student's *t* test.

(H and I) Low-frequency PFC activation decreased the aversive response to noxious stimulation. One of the chambers was paired with 2-Hz stimulation of the PFC and noxious stimulus; the other chamber was paired with the noxious stimulus without PFC activation. YFP-treated rats demonstrated no preference for either chamber. $n = 8$, $p = 0.7745$, paired Student's *t* test (H). In contrast, ChR2-treated rats spent more time during the test phase than at baseline in the chamber-paired associated with PFC activation. $n = 10$, $p < 0.0001$, paired Student's *t* test (I).

(J) Low-frequency PFC activation decreased the CPA score. $n = 8$ – 10 , $p = 0.0118$, unpaired Student's *t* test.

(K and L) Low-frequency PFC activation decreased the aversive response to noxious stimulation. One of the chambers was paired with 2 Hz stimulation of the PFC and PP; the other chamber was not paired with an acute pain stimulus (NS). YFP-treated rats displayed preference for the no-pain chamber. $n = 9$, $p = 0.0021$, paired Student's *t* test (K). In contrast, ChR2-treated rats displayed no preference for either chamber. $n = 10$, $p = 0.9473$, paired Student's *t* test (L).

(M) Low-frequency PFC activation decreased the aversive response to noxious stimulation, which was demonstrated by diminished CPA score. $n = 9$ – 10 , $p = 0.0195$, unpaired Student's *t* test.

(N and O) Low-frequency PFC stimulation decreased the aversive response to PP in CFA-treated rats. CFA-treated rats underwent the same CPA test as in (H)–(J), with noxious stimulation in the uninjured paw. YFP-treated rats demonstrated no preference. $n = 8$, $p = 0.8402$, paired Student's *t* test (N). In contrast, ChR2-treated rats preferred the chamber paired with PFC activation. $n = 10$, $p = 0.0027$, paired Student's *t* test (O).

(P) Low-frequency PFC activation decreased the aversive response to noxious stimulation in the chronic pain state. $n = 8$ – 10 , $p = 0.0175$, unpaired Student's *t* test.

(Q and R) Low-frequency PFC activation decreased the aversive response to noxious stimulation in CFA-treated rats. CFA-treated rats underwent the same CPA test as in (K)–(M), with stimulation in the uninjured paws. YFP-treated rats displayed preference for the no-pain chamber. $n = 8$, $p = 0.0006$, paired Student's *t* test (Q). In contrast, ChR2-treated rats displayed no preference. $n = 10$, $p = 0.0889$, paired Student's *t* test (R).

(S) Low-frequency PFC activation decreased the aversive response to noxious stimulation in the chronic pain state. $n = 8$ – 10 , $p = 0.0147$, unpaired Student's *t* test. All of the data are presented as means \pm SEMs.

See also Figures S3–S5.

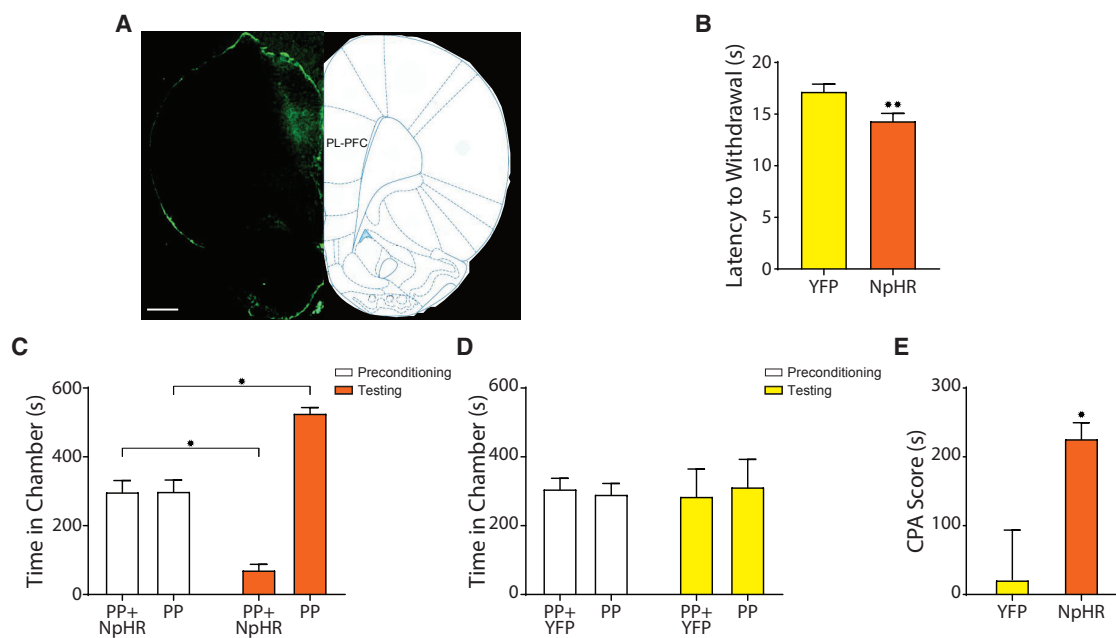


Figure 5. Inhibition of the PL-PFC Enhances Both Sensory and Affective Components of Pain

(A) Expression of halorhodopsin from *Natronomonas* (NpHR)-eYFP in the PL-PFC. Scale bar, 1,000 μ m.

(B) Optogenetic inhibition of the PFC decreased the latency to paw withdrawal on the Hargreaves test. $n = 9-11$, $p = 0.0081$, unpaired Student's *t* test.

(C) Inhibition of the PFC increased the aversive response to acute pain. During the conditioning phase of the CPA, one of the chambers was paired with optogenetic inhibition of the PFC and peripheral noxious stimulation (PP); the other chamber was paired with PP without PFC inhibition. NpHR-treated rats demonstrated avoidance of the chamber associated with optogenetic inhibition. $n = 7$, $p = 0.0263$, paired Student's *t* test.

(D) YFP-treated rats did not show any preference for or avoidance of either chamber. $n = 8$, $p = 0.7745$, paired Student's *t* test.

(E) Inhibition of PL-PFC increased the aversive response to acute pain, as demonstrated by an increased CPA score in NpHR-treated rats compared with YFP-treated rats. $n = 7-8$, $p = 0.0239$, unpaired Student's *t* test.

All of the data are presented as means \pm SEMs.

(Figures S5A and S5B). This corticostriatal projection has been shown to be a specific pathway for descending pain control (Lee et al., 2015; Martinez et al., 2017). We found that 2-Hz stimulation of the PFC neurons that project to the NAc core prolonged the latency to withdrawal on the Hargreaves test, demonstrating anti-nociceptive effects (Figure S5C). Next, we showed that scaling up the prefrontal output to the NAc also could provide relief of mechanical allodynia in CFA-treated rats (Figure S5D). Finally, we used the CPA test to investigate the impact of scaling up this corticostriatal pathway on the affective pain symptoms. We paired PP with 2-Hz activation of PFC neurons that project to the NAc in one chamber and PPs without optogenetic activation in the opposite chamber during conditioning. During the test phase, rats preferred the chamber associated with corticostriatal activation (Figures S5E–S5G). These data indicate that enhancing the gain of PFC neurons that are known to provide descending inhibition can regulate pain-related behaviors.

DISCUSSION

In this study, we present a mechanism of cortical gain control for nociceptive processing. This cortical gain control mechanism links intrinsic cellular excitability within the PFC with the strength of cortical regulatory networks. We found that chronic pain de-

creases this cortical gain to reduce endogenous nociceptive regulation. Conversely, based on this gain control mechanism, we designed a neuromodulation strategy that uses low-frequency stimulation to specifically enhance basal activities in the PFC within the physiologic range to amplify its regulatory outputs and inhibit pain-triggered behaviors.

The PFC is known to provide top-downregulation for a variety of sensory and affective processes (Salzman and Fusi, 2010). Our study presents the first detailed evidence of how neurons in the PFC respond to acute pain signals in awake, free-moving animals. In our study, we found a marked difference in the latency, duration, and magnitude of spike responses between painful and non-painful stimuli. The population-decoding analysis further supports the relative specificity of the prefrontal response to pain. It should be noted, however, that our results do not necessarily prove that there are specific pain-processing neurons versus pain-regulatory neurons in the PFC. Rather, our results demonstrate that the response to nociceptive inputs is one of the key roles performed by neurons in the PFC. Indeed, prefrontal neurons have been shown to exhibit mixed selectivity during various behavioral tasks (Rigotti et al., 2013). The specific function of PFC at a given time may thus depend on the precise behavioral context. In the presence of an acute pain signal, a number of neurons in the PFC will increase their FRs to project to regions such as the NAc to inhibit pain. In the presence of a

different sensory cue such as light touch or sound, the same or different PFC neurons may exhibit different spiking patterns and project to other brain regions to drive different sets of behaviors. When the optogenetic activation was coupled with a pain stimulus in our study, it was able to activate further those pain-responsive neurons to inhibit pain. Conversely, inhibition of these PFC neurons resulted in a lack of endogenous regulation and subsequently increased pain. Hence, our results provide a crucial physiological basis for previous data showing the ability of PFC stimulation to inhibit pain (Hardy, 1985; Kiritoshi et al., 2016; Lee et al., 2015; Martinez et al., 2017; Zhang et al., 2015). In addition, our results demonstrate for the first time that chronic pain suppresses the prefrontal response to nociceptive inputs at the population level and the level of individual neurons.

The concept of gain control for nociceptive processing has been documented in peripheral and spinal systems, and mechanisms such as gate control and central sensitization provide bases for understanding pain amplification and inhibition (Melzack and Wall, 1965; Treede, 2016). However, details of a cortical gain control mechanism have remained elusive. In this study, we demonstrated that the PFC is an important center for cortical gain control. The PFC has the ability to inhibit both sensory and affective pain signals by descending projections to the striatum, amygdala, brainstem, and spinal cord (Fields et al., 1983; Ji and Neugebauer, 2014; Lee et al., 2015). Thus, increasing the gain in the PFC provides increased nociceptive control. Chronic pain, however, causes hypoexcitability of PFC neurons (Ji and Neugebauer, 2011, 2014; Kelly et al., 2016; Kiritoshi et al., 2016; Radzicki et al., 2017). This prefrontal gain control mechanism provides a link between cellular hypoexcitability and deficient nociceptive regulation at the systems level. Because evoked FRs are a linear multiple of basal FRs, even a small decrease in basal excitability can result in a nearly 2-fold deficit in prefrontal outputs to descending inhibitory pathways. Therefore, a reduction in the gain of prefrontal control is an important mechanism for chronic pain.

Previous reports suggest that cortical neurons can preserve their scale of activity levels across different behavioral states, including sleep (Buzsáki and Mizuseki, 2014; Stark et al., 2015). Thus, it will be interesting to apply our findings of nociceptive processing to other sensory and affective inputs. Specifically, we speculate that chronic pain also can scale down prefrontal responses to non-nociceptive sensory and affective inputs to give rise to depression, altered reward processing, and anxiety, which often are associated with pain. More generally, our study raises the question of whether downscaling of cortical operations is a general feature of neuropsychiatric diseases.

The most important finding in our study is that the cortical gain control mechanism provides the basis for a novel approach to neuromodulation. Traditional designs of neuromodulation rely on high-frequency, supraphysiologic stimulation to either activate or inhibit neurons in a specific brain region (Ashkan et al., 2017; De Ridder et al., 2017; Levy et al., 1987). Applications of this method to the PFC have been effective in pain relief in animal models (Lee et al., 2015; Martinez et al., 2017; Wang et al., 2015). Our behavior results indicate that using low-frequency stimula-

tion to scale up cortical outputs also has the potential to inhibit both sensory and affective pain components. This novel neuromodulation strategy aims to optimize endogenous cortical functions, rather than to hijack the native cortical circuitry. This approach has the potential to inhibit pain while minimizing adverse effects, and it would be interesting to generalize this strategy to other neuropsychiatric conditions. It is important to note that the basis for cortical gain control is that basal activities of the PFC neurons can be enhanced to increase the prefrontal response to a noxious stimulus. This mechanism is not limited to low-frequency invasive stimulations. In fact, low-intensity noninvasive stimulation methods such as transcranial current stimulation (tCS) are known to elevate the basal firing of cortical neurons. tCS is relatively safe, and it is being investigated in a number of disease conditions, including recovery of motor functions after stroke (Schlaug et al., 2008). Therefore, our results provide an important mechanism for these non-invasive neuromodulation methods and support their investigation in patients with chronic pain.

The PFC is part of a complex cortical network for nociceptive processing. It receives inputs from the primary somatosensory cortex (S1). We and others have found that in contrast to neurons in the PFC, S1 neurons can be both excited and inhibited by noxious stimulations (Chen et al., 2017; Kuo and Yen, 2005; Vierck et al., 2013; Zhang et al., 2011). The PFC also receives inputs from and in turn projects to neurons in the ACC. Like the PFC, ACC neurons mostly increase their FRs in response to pain (Chen et al., 2017; Kuo and Yen, 2005; Zhang et al., 2011). The PFC and ACC are centers in the medial affective pain pathway, whereas the S1 is a component in the lateral sensory pathway. These differences in firing rate responses in the S1, and ACC and PFC suggest distinct pain coding schemes in the medial and lateral pathways. Within the medial pathway, there also are important differences. Chronic pain increases ACC responses to acute pain (Chen et al., 2017; Zhang et al., 2017), leading to a generalized anatomically nonspecific form of enhancement in pain aversion that is well described in the clinical literature (Kudel et al., 2007; Li et al., 2010; Petzke et al., 2003; Xu et al., 2008; Zhang et al., 2017). In contrast, chronic pain decreases the functions of the PFC to contribute to this generalized enhancement of aversion. Comparisons with S1 and ACC neurons support the specificity of the nociceptive response in PFC neurons and further indicate that different regions in the brain can be either scaled up or down by chronic pain. Cortical pain-processing centers are known to mutually inhibit or excite one another, depending on the behavioral context (Ji and Neugebauer, 2012; Riga et al., 2014). Therefore, neuromodulation strategies to alter gain control also can affect cortico-cortical dynamics in the chronic pain state.

In summary, neurons in the PFC increase their FRs in response to noxious stimulations and have the potential to function as gain controllers for pain. Chronic pain decreases basal FRs to scale down the prefrontal response to acute pain, resulting in depressed nociceptive regulation. Low-frequency stimulation, in contrast, can enhance cortical control to be an effective treatment strategy to inhibit pain and possibly other neuropsychiatric diseases.

EXPERIMENTAL PROCEDURES

Animals

All of the procedures were performed in accordance with the guidelines of the New York University School of Medicine (NYUSOM) Institutional Animal Care and Use Committee (IACUC), as consistent with the NIH *Guide for the Care and Use of Laboratory Animals* to ensure minimal animal use and discomfort. Male Sprague-Dawley rats were purchased from Taconic Farms and kept at Mispro Biotech Services facility in the Alexandria Center for Life Science, with controlled humidity, temperature, and 12-hr (6:30 AM–6:30 PM) light-dark cycle. Food and water were available ad libitum. Animals arrived at the animal facility weighing 250 to 300 g and were given on average 10 days to adjust to the new environment before the initiation of experiments.

CFA Administration

To induce chronic inflammatory pain, 0.1 mL of CFA (*Mycobacterium tuberculosis*, Sigma-Aldrich) was suspended in an oil:saline (1:1) emulsion and injected subcutaneously into the plantar aspect of the hind paw opposite to the paw that was stimulated by PP. CFA always was administered into the paw that was ipsilateral to the recording electrodes. Control rats received an equal volume of saline injection.

Virus Construction and Packaging

Recombinant adeno-associated virus (AAV) vectors were serotyped with AAV1 coat proteins and packaged at the University of Pennsylvania Vector Core. Viral titers were 5×10^{12} particles per milliliter for AAV1.CaMKII. ChR2-eYFP.WPRE.hGH, AAV1.CaMKII.NpHR-eYFP.WPRE.hGH, and AAV1.CaMKII(1.3).eYFP.WPRE.hGH.

Stereotaxic Intracranial Injections and Optic Fiber Implantation

As described previously (Lee et al., 2015), rats were anesthetized with isoflurane (1.5%–2%). In all of the experiments, virus was delivered to the PL-PFC only. Rats were bilaterally injected with 0.6 μ L viral vectors at a rate of 0.1 μ L/10 s with a 26G 1 μ L Hamilton syringe at anteroposterior (AP) +2.9 mm, mediolateral (ML) \pm 1.6 mm, and dorsoventral (DV) –3.7 mm, with tips angled 12.5° toward the midline. Rats were then implanted with 200- μ m optic fibers held in 1.25 mm ferrules (Thorlabs) in the PL-PFC (AP +2.9 mm, ML \pm 1.6 mm, DV –2.7 mm) or in the NAC core (AP +2.2 mm, ML \pm 2.8 mm, DV –5.7 mm with tips angled 12° toward the midline). Fibers with ferrules were held in place by dental acrylic.

Electrode Implant and Surgery

Tetrodes were constructed from four twisted 12.7 μ m polyimide-coated micro-wires (Sandvik) and mounted in an eight-tetrode VersaDrive (Neuralynx). Electrode tips were plated with gold to reduce electrode impedances to 100–500 k Ω at 1 kHz. Rats were anesthetized with isoflurane (1.5%–2%). The skull was exposed and a 3 mm-diameter hole was drilled above the target region. A durotomy was performed before tetrodes were slowly lowered unilaterally into the PL-PFC with the stereotaxic apparatus. The coordinates for PL-PFC tetrode implants were AP +3.2 mm, ML +1.4 mm, and DV –2.5 mm, with tetrode tips angled 13° toward the midline. The drive was secured to the skull screws with dental cement.

After animal sacrifice, brain sections (20 μ m) were collected using a Microm HM525 cryostat machine (Thermo Fisher Scientific) and analyzed for viral expression and optic fiber localization with histological staining. Animals with improper fiber or electrode placements, low viral expression, or viral expression outside the PL-PFC were excluded from further analysis.

Chronic Optrode Implant and Intracranial Injections

Tetrodes were constructed from four twisted 12.7 μ m polyimide-coated micro-wires (Sandvik) and mounted in an eight-tetrode VersaDrive Optical (Neuralynx). A 200 μ m optic fiber held in 1.25 mm ferrules (Thorlabs) were mounted in the VersaDrive Optical such that the fiber was 0.5–1 mm above the mounted tetrodes. Electrode tips were plated with gold to reduce electrode impedances to 100–500 k Ω at 1 kHz. Rats were anesthetized with isoflurane (1.5%–2%). The skull was exposed and a 3 mm-diameter hole was drilled above the target region. A durotomy was performed before rats

were unilaterally injected with 0.6 μ L viral vectors at a rate of 0.1 μ L/10 s with a 26G 1 μ L Hamilton syringe at AP +3.2 mm, ML +1.4 mm, and DV –3 mm, with tips angled 13° toward the midline. Optrodes were slowly lowered unilaterally into the PL-PFC with the stereotaxic apparatus. The coordinates for PL-PFC optrode implants were AP +3.2 mm, ML +1.4 mm, and DV –3 mm, with tetrode tips angled 13° toward the midline. The drive was secured to the skull screws with dental cement.

In Vivo Electrophysiological Recordings

As described previously, before stimulation, animals with chronic tetrode implants were given 30 min to habituate to a recording chamber over a mesh table (Zhang et al., 2017). Noxious stimulation by pricking with a 28G needle (PP) was applied to the plantar surface of the hind paw contralateral to the brain recording site in free-moving rats. Noxious stimulation was terminated by paw withdrawals. Non-noxious stimulus using 2 g VF filament was applied to the hind paws. In a majority of cases, there were no withdrawals in response to VF filaments, and VF filament was continuously applied for 3 s or until withdrawal. All of the recording sessions consisted of approximately 60 trials with variable intertrial intervals. Recording sessions used both PP and VF filament stimulation. The stimulations were applied randomly to rat's hind paws for approximately 60 trials (equal number of trials for each stimulation type). A video camera (HC-V550, Panasonic) was used to record the experiment. Long intertrial intervals and the breaks between sessions were used to avoid sensitization. No behavioral sensitization or physical damage to the paws was observed.

Animals with optrode implants were given 30 min to habituate to a recording chamber over a mesh table. Animals were given PP stimulation with approximately 60 trials of variable intertrial intervals. Thirty consecutive trials would be conducted either with or without constant 2 Hz optogenetic stimulation. Another 30 trials would be conducted under the opposite condition to complete a recording session. Because of the design of the optrodes, where the recording tetrodes surround the central optic fiber, light through the optic fiber could activate only approximately half of the neurons recorded from the tetrodes.

Neural Data Collection and Preprocessing

Tetrodes were lowered in steps of 60 μ m before each day of recording. The neuronal activity and the onset of PP stimulation were simultaneously recorded with acquisition equipment (Open Ephys) via an RHD2132 amplifier board (Intan Technologies). Signals were monitored and recorded from 32 low-noise amplifier channels at 30 kHz, band-pass filtered (0.3–7.5 kHz). To achieve spike activity, the raw data were high-pass filtered at 300 Hz with subsequent thresholding and offline sorting by commercial software (Offline Sorter, Plexon). The threshold was lower than the 3-sigma peak heights line and optimized manually based on the signal-to-noise ratio. The features of three valley electrodes were used for spike sorting. Trials were aligned to the initiation of the peripheral stimulus to compute the peristimulus time histogram (PSTH) for each single unit using MATLAB (MathWorks).

Immunohistochemistry

Rats were anesthetized deeply with isoflurane and transcardially perfused with ice-cold PBS. Brains were fixed in paraformaldehyde (PFA) overnight and then transferred to 30% sucrose in PBS to equilibrate for 3 days as described (Lee et al., 2015). Coronal sections, 20 μ m, were washed in PBS and coverslipped with Vectashield mounting medium. Images containing tetrodes were stained with cresyl violet and viewed and recorded under a Nikon Eclipse 80i microscope with a DS-U2 camera head. Sections also were made after viral transfer for opsin verification, and these sections were stained with anti-rabbit GFP (1:500, #AB290, Abcam), CaMKII- α (6G9) mouse monoclonal antibody (mAb) (1:100, #50049, Cell Signaling Technology), and DAPI (1:200, Vector Laboratories) antibodies. Secondary antibodies were anti-rabbit immunoglobulin G (IgG) conjugated to Alexa Fluor 488, and anti-mouse IgG conjugated to Alexa Fluor 647 (1:200, Life Technologies). Images were acquired with a Zeiss LSM 700 confocal microscope (Carl Zeiss).

Animal Behavioral Tests

For optogenetic experiments, optic fibers were connected to a 473 nm (for channelrhodopsin-2 [ChR2]) laser diode (Shanghai Dream Lasers Technology)

through a mating sleeve, as described by Lee et al. (2015). Laser was delivered using a transistor-transistor logic (TTL) pulse generator (Doric Lenses).

CPA

CPA experiments were conducted similar to what was described by Zhang et al. (2017). The movements of animals in each chamber were recorded by a camera and analyzed with ANY-maze software. The CPA protocol included preconditioning (baseline), conditioning, and testing phases (10 min during each phase). Animals spending >500 s or <100 s of the total time in either main chamber in the preconditioning phase were eliminated from further analysis. Immediately following the preconditioning phase, the rats underwent conditioning for 10 min. During conditioning, one of the two chambers was paired with PP. The PP stimulus was repeated every 10 s. During the optogenetic experiments, constant 2 Hz optogenetic activation was applied to one of the treatment chambers during the conditioning phase only. Peripheral stimulation, optogenetic activation, and chamber pairings were counterbalanced. During the test phase, the animals did not receive any treatment and had free access to both compartments for a total of 10 min. Animal movements in each of the chambers were recorded, and the time spent in either of the treatment chambers was analyzed by ANY-maze software. Decreased time spent in a chamber during the test phase as compared with the baseline indicated avoidance (aversion) of that chamber.

Mechanical Allodynia Test

A Dixon up-down method with VF filaments was used to measure mechanical allodynia (Lee et al., 2015). Rats were placed individually into plexiglass chambers over a mesh table and acclimated for 20 min before testing. Beginning with 2.55 g, VF filaments in a set with logarithmically incremental stiffness (0.45, 0.75, 1.20, 2.55, 4.40, 6.10, 10.50, and 15.10 g) were applied to the paws of rats. A 50% withdrawal threshold was calculated, as described previously (Lee et al., 2015).

Hargreaves Test (Plantar Test)

The Hargreaves test was performed to evaluate the response to acute thermal stimulation (Lee et al., 2015). A mobile radiant heat-emitting device with an aperture of 10 mm (37370 Plantar Test, Ugo Basile) was used to produce acute thermal stimulation of the plantar surface of the hind paw. The latency to paw withdrawal was automatically recorded. Paw withdrawals resulting from locomotion or weight shifting were not counted and the trials were repeated. Measurements were repeated five times at 5 min intervals.

Statistical Analysis

The results of behavioral experiments were given as means \pm SEMs. A two-tailed paired Student's *t* test was used to analyze the results from the Hargreaves test. For mechanical allodynia, a two-way ANOVA with repeated-measures and post hoc multiple pairwise comparison Bonferroni tests or unpaired *t* tests were used whenever appropriate. During the CPA test, a paired Student's *t* test was used to compare the time spent in each treatment chamber before and after conditioning (i.e., baseline versus test phase for each chamber). Decreased time spent in a chamber during the test phase as compared with the baseline indicated avoidance (aversion) of that chamber. A CPA score was computed by subtracting the time spent in the more noxious chamber during the test phase from the time spent in that chamber at baseline (Johansen et al., 2001). A two-tailed unpaired Student's *t* test was used to compare differences in CPA scores under various testing conditions.

For neuronal spike analysis, we calculated PSTHs using a 5-s range before and after peripheral stimulus (i.e., PP or VF filament) and a bin size of 100 ms. The number of spikes in each stimulus-aligned bin was averaged across all of the trials to create the PSTH. We then calculated the basal spontaneous firing rate for each neuron to be the average of the PSTH bins before stimulus onset and the peak pain-evoked firing rate to be the maximum value of the PSTH after stimulus onset (within 5 s from the stimulus). We also used a linear regression model to fit the baseline mean FRs versus the peak pain-evoked FRs.

To define a neuron that altered its firing rate in response to a peripheral stimulus, we used the method described by Zhang et al. (2017). The baseline mean is the average of the PSTH bins before stimulus onset, and the standard deviation is the standard deviation of the PSTH bins before stimulus

onset. To calculate the *Z* scored firing rate, we used the following equation: $Z = (FR - \text{mean of } FR_b) / \text{standard deviation of } FR_b$, where *FR* indicates the firing rate for each bin and *FR_b* indicates the baseline firing rate before stimulus onset. To define a pain-responsive neuron, we used the following criteria: (1) the absolute value of the *Z* scored firing rate of at least one time bin after stimulation must be ≥ 2.5 , and (2) if the first criterion is passed, at least the next two bins must be >1.645 . These criteria must be fulfilled within 3 s after the peripheral stimulus.

Neuronal FRs had a non-Gaussian distribution, compatible with a previous report (Buzsáki and Mizuseki, 2014). Thus, nonparametric tests were performed. For unpaired data, a Mann-Whitney *U* test was performed to test the equivalence of distributions. The Wilcoxon matched-pairs signed-rank test was used to test the equivalence of distributions for paired data. Fisher's exact test was used to analyze the population changes for pain response. In these studies, because of the negligible number of neurons that decreased their FRs in response to stimulation (PP or VF filament), we included those neurons in the category of non-responders.

For all tests, a *p* value < 0.05 was considered statistically significant. All of the data were analyzed using GraphPad Prism version 7 software and MATLAB (MathWorks).

Population-Decoding Analysis Using Machine Learning

After spike sorting, we obtained population spike trains from simultaneously recorded PFC neurons. For each single neuronal recording, we binned spikes into 50 ms to obtain spike count data in time. To simulate the online decoding, we used a 50-ms moving window to accumulate spike count statistics from the onset of the peripheral stimulus (time 0) up to 3 s (i.e., 60 bins). We assessed the decoding accuracy at each time bin based on the cumulative spike count statistics. Therefore, for a total of *C* neurons, the input dimensionality ranged from *C* (the first bin) to 60*C* (all bins). In these experiments in which we randomly mixed different stimulations (PP and VF filament), we assumed that we had *n*₁ trials of PP and *n*₂ trials of VF filament. We split the total (*n*₁ + *n*₂) trials into two groups: 80% used for training and 20% used for testing. The goal of population-decoding analysis was to classify the trial labels of different stimulations (PP versus VF filament) based on population spike data. We used an SVM classifier (Bishop, 2007). The SVM is a discriminative supervised learning model that constructs the classification boundary by a separating hyperplane with maximum margin. Specifically, the SVM can map the input *x* into high-dimensional feature spaces, which allows nonlinear classification, as follows:

$$y = \sum_{i=1}^N \alpha_i K(\mathbf{x}, \mathbf{x}_i) + b,$$

where $y_i \in \{-1, +1\}$ denotes the class label for the training sample \mathbf{x}_i (some of which associated with nonzero α_i are called support vectors), *b* denotes the bias, and $K(\mathbf{x}, \mathbf{x}_i)$ denotes the kernel function. We used a polynomial kernel and trained the nonlinear SVM with a sequential minimal optimization algorithm (MATLAB Machine Learning Toolbox "fitcsvm" function). Finally, the decoding accuracy was assessed by 5-fold cross-validation from 50 Monte Carlo simulations. We reported the means \pm SEMs. In all of the population-decoding analyses, we used only the 20 recording sessions with ≥ 5 simultaneously recorded PFC units, independent of the cell-firing properties.

SUPPLEMENTAL INFORMATION

Supplemental Information includes five figures and can be found with this article online at <https://doi.org/10.1016/j.celrep.2018.03.139>.

ACKNOWLEDGMENTS

The work was supported by NIH grants GM115384 (to J.W.) and NS100065 (to Z.C. and J.W.), National Science Foundation-Collaborative Research in Computational Neuroscience (NSF-CRCNS) grant IIS-130764 (to Z.C.), the National Natural Science Foundation of China (81771101 to H.Z.), and the China Scholarship Council (201606370208 to H.Z.).

AUTHOR CONTRIBUTIONS

J.D., H.Z., Z.C., and J.W. designed the experiments. J.D., H.Z., Q.Z., and S.H. performed the electrophysiological recording experiments. J.D., H.Z., E.M., K.L., and L.U. performed the behavior testing. J.D., H.Z., and Q.Z. performed the statistical analysis. J.W. wrote the manuscript.

DECLARATION OF INTERESTS

The authors declare no competing interests.

Received: October 8, 2017

Revised: February 23, 2018

Accepted: March 29, 2018

Published: May 1, 2018

REFERENCES

- Apkarian, A.V., Sosa, Y., Sonty, S., Levy, R.M., Harden, R.N., Parrish, T.B., and Gitelman, D.R. (2004). Chronic back pain is associated with decreased prefrontal and thalamic gray matter density. *J. Neurosci.* *24*, 10410–10415.
- Ashkan, K., Rogers, P., Bergman, H., and Ughratdar, I. (2017). Insights into the mechanisms of deep brain stimulation. *Nat. Rev. Neurol.* *13*, 548–554.
- Basbaum, A.I., Bautista, D.M., Scherrer, G., and Julius, D. (2009). Cellular and molecular mechanisms of pain. *Cell* *139*, 267–284.
- Bishop, C. (2007). *Pattern Recognition and Machine Learning* (Springer).
- Buzsáki, G., and Mizuseki, K. (2014). The log-dynamic brain: how skewed distributions affect network operations. *Nat. Rev. Neurosci.* *15*, 264–278.
- Chen, Z., Zhang, Q., Tong, A.P.S., Manders, T.R., and Wang, J. (2017). Deciphering neuronal population codes for acute thermal pain. *J. Neural Eng.* *14*, 036023.
- De Ridder, D., Perera, S., and Vanneste, S. (2017). State of the art: novel applications for cortical stimulation. *Neuromodulation* *20*, 206–214.
- Fields, H.L., Bry, J., Hentall, I., and Zorman, G. (1983). The activity of neurons in the rostral medulla of the rat during withdrawal from noxious heat. *J. Neurosci.* *3*, 2545–2552.
- Geha, P.Y., Baliki, M.N., Harden, R.N., Bauer, W.R., Parrish, T.B., and Apkarian, A.V. (2008). The brain in chronic CRPS pain: abnormal gray-white matter interactions in emotional and autonomic regions. *Neuron* *60*, 570–581.
- Hardy, S.G. (1985). Analgesia elicited by prefrontal stimulation. *Brain Res.* *339*, 281–284.
- Ji, G., and Neugebauer, V. (2011). Pain-related deactivation of medial prefrontal cortical neurons involves mGluR1 and GABA(A) receptors. *J. Neurophysiol.* *106*, 2642–2652.
- Ji, G., and Neugebauer, V. (2012). Modulation of medial prefrontal cortical activity using in vivo recordings and optogenetics. *Mol. Brain* *5*, 36.
- Ji, G., and Neugebauer, V. (2014). CB1 augments mGluR5 function in medial prefrontal cortical neurons to inhibit amygdala hyperactivity in an arthritis pain model. *Eur. J. Neurosci.* *39*, 455–466.
- Johansen, J.P., Fields, H.L., and Manning, B.H. (2001). The affective component of pain in rodents: direct evidence for a contribution of the anterior cingulate cortex. *Proc. Natl. Acad. Sci. USA* *98*, 8077–8082.
- Kelly, C.J., Huang, M., Meltzer, H., and Martina, M. (2016). Reduced glutamatergic currents and dendritic branching of layer 5 pyramidal cells contribute to medial prefrontal cortex deactivation in a rat model of neuropathic pain. *Front. Cell. Neurosci.* *10*, 133.
- King, T., Vera-Portocarrero, L., Gutierrez, T., Vanderah, T.W., Dussor, G., Lai, J., Fields, H.L., and Porreca, F. (2009). Unmasking the tonic-aversive state in neuropathic pain. *Nat. Neurosci.* *12*, 1364–1366.
- Kiritoshi, T., Ji, G., and Neugebauer, V. (2016). Rescue of impaired mGluR5-driven endocannabinoid signaling restores prefrontal cortex output to inhibit pain in arthritic rats. *J. Neurosci.* *36*, 837–850.
- Kudel, I., Edwards, R.R., Kozachik, S., Block, B.M., Agarwal, S., Heinberg, L.J., Haythornthwaite, J., and Raja, S.N. (2007). Predictors and consequences of multiple persistent postmastectomy pains. *J. Pain Symptom Manage.* *34*, 619–627.
- Kuo, C.C., and Yen, C.T. (2005). Comparison of anterior cingulate and primary somatosensory neuronal responses to noxious laser-heat stimuli in conscious, behaving rats. *J. Neurophysiol.* *94*, 1825–1836.
- Lee, M., Manders, T.R., Eberle, S.E., Su, C., D'amour, J., Yang, R., Lin, H.Y., Deisseroth, K., Froemke, R.C., and Wang, J. (2015). Activation of corticostriatal circuitry relieves chronic neuropathic pain. *J. Neurosci.* *35*, 5247–5259.
- Levy, R.M., Lamb, S., and Adams, J.E. (1987). Treatment of chronic pain by deep brain stimulation: long term follow-up and review of the literature. *Neurosurgery* *21*, 885–893.
- Li, X.Y., Ko, H.G., Chen, T., Descalzi, G., Koga, K., Wang, H., Kim, S.S., Shang, Y., Kwak, C., Park, S.W., et al. (2010). Alleviating neuropathic pain hypersensitivity by inhibiting PKMzeta in the anterior cingulate cortex. *Science* *330*, 1400–1404.
- Martinez, E., Lin, H.H., Zhou, H., Dale, J., Liu, K., and Wang, J. (2017). Corticostriatal regulation of acute pain. *Front. Cell. Neurosci.* *11*, 146.
- Melzack, R., and Wall, P.D. (1965). Pain mechanisms: a new theory. *Science* *150*, 971–979.
- Moayed, M., Weissman-Fogel, I., Crawley, A.P., Goldberg, M.B., Freeman, B.V., Tenenbaum, H.C., and Davis, K.D. (2011). Contribution of chronic pain and neuroticism to abnormal forebrain gray matter in patients with temporomandibular disorder. *Neuroimage* *55*, 277–286.
- Navratilova, E., Xie, J.Y., Okun, A., Qu, C., Eyde, N., Ci, S., Ossipov, M.H., King, T., Fields, H.L., and Porreca, F. (2012). Pain relief produces negative reinforcement through activation of mesolimbic reward-valuation circuitry. *Proc. Natl. Acad. Sci. USA* *109*, 20709–20713.
- Petzke, F., Clauw, D.J., Ambrose, K., Khine, A., and Gracely, R.H. (2003). Increased pain sensitivity in fibromyalgia: effects of stimulus type and mode of presentation. *Pain* *105*, 403–413.
- Radzicki, D., Pollema-Mays, S.L., Sanz-Clemente, A., and Martina, M. (2017). Loss of M1 receptor dependent cholinergic excitation contributes to mPFC deactivation in neuropathic pain. *J. Neurosci.* *37*, 2292–2304.
- Riga, D., Matos, M.R., Glas, A., Smit, A.B., Spijker, S., and Van den Oever, M.C. (2014). Optogenetic dissection of medial prefrontal cortex circuitry. *Front. Syst. Neurosci.* *8*, 230.
- Rigotti, M., Barak, O., Warden, M.R., Wang, X.J., Daw, N.D., Miller, E.K., and Fusi, S. (2013). The importance of mixed selectivity in complex cognitive tasks. *Nature* *497*, 585–590.
- Salzman, C.D., and Fusi, S. (2010). Emotion, cognition, and mental state representation in amygdala and prefrontal cortex. *Annu. Rev. Neurosci.* *33*, 173–202.
- Schlaug, G., Renga, V., and Nair, D. (2008). Transcranial direct current stimulation in stroke recovery. *Arch. Neurol.* *65*, 1571–1576.
- Stark, E., Roux, L., Eichler, R., and Buzsáki, G. (2015). Local generation of multineuronal spike sequences in the hippocampal CA1 region. *Proc. Natl. Acad. Sci. USA* *112*, 10521–10526.
- Treede, R.D. (2016). Gain control mechanisms in the nociceptive system. *Pain* *157*, 1199–1204.
- Vierck, C.J., Whitsel, B.L., Favorov, O.V., Brown, A.W., and Tommerdahl, M. (2013). Role of primary somatosensory cortex in the coding of pain. *Pain* *154*, 334–344.
- Wang, G.Q., Cen, C., Li, C., Cao, S., Wang, N., Zhou, Z., Liu, X.M., Xu, Y., Tian, N.X., Zhang, Y., et al. (2015). Deactivation of excitatory neurons in the prefrontal cortex via Cdk5 promotes pain sensation and anxiety. *Nat. Commun.* *6*, 7660.

Xu, H., Wu, L.J., Wang, H., Zhang, X., Vadakkan, K.I., Kim, S.S., Steenland, H.W., and Zhuo, M. (2008). Presynaptic and postsynaptic amplifications of neuropathic pain in the anterior cingulate cortex. *J. Neurosci.* *28*, 7445–7453.

Zhang, Y., Wang, N., Wang, J.Y., Chang, J.Y., Woodward, D.J., and Luo, F. (2011). Ensemble encoding of nociceptive stimulus intensity in the rat medial and lateral pain systems. *Mol. Pain* *7*, 64.

Zhang, Z., Gadotti, V.M., Chen, L., Souza, I.A., Stemkowski, P.L., and Zamponi, G.W. (2015). Role of prelimbic GABAergic circuits in sensory and emotional aspects of neuropathic pain. *Cell Rep.* *12*, 752–759.

Zhang, Q., Manders, T., Tong, A.P., Yang, R., Garg, A., Martinez, E., Zhou, H., Dale, J., Goyal, A., Urien, L., et al. (2017). Chronic pain induces generalized enhancement of aversion. *eLife* *6*, e25302.